Resolution of the Hall–Petch equation and comparison with the experimental results of three vanadium–titanium microalloyed steels

M. CARSÍ
CENIM, Avda. Gregario del Amo, 8, Madrid, 28040, Spain

F. PENALBA
INASMET, San Sebastian, Spain

I. GUTIÉRREZ
CEIT, San Sebastian, Spain

Results obtained when increasing quantities of titanium are added to a vanadium microalloyed steel are reported. Starting with the TEM study of the particles and pearlite, the theoretical equations of Gladman, Kouwenhoven, Licka and Burnett were applied to a connecting rod manufactured with three medium carbon steels in order to calculate the yield strength and the impact transition temperature (ITT). Through a comparison of the theoretical and experimental results, it was concluded that Gladman's equation is the best equation for obtaining more realistic results in this kind of microalloyed steel.

1. Introduction

This paper forms part of a more extensive work [1] carried out on medium carbon steels, microalloyed with vanadium and titanium (titanium varies from 0.003%–0.039% by weight). The present work study evaluated the influence of the additions of vanadium and titanium on microalloyed steels properties, such as continuous cooling diagrams, hot and warm ductility, grain growth, static and dynamic recrystallization, etc., and the influence of both hot and warm forging parameters on the structures and properties of forged critical automotive components, with a view to improving the toughness properties. This would be achieved because the vanadium and titanium–vanadium precipitates would control the degree of grain growth and the recrystallized austenitic grain size. These precipitates (vanadium and titanium carbonitrides and nitrides) made it possible to reduce the size of the ferritic–pearlitic grain obtained after the transformation during cooling at almost air-cooling rates.

The present work focuses on determining the size and distribution of nitrides and carbonitrides from two forging sequences. The experimental results have been compared with those provided by the theoretical provisions made through the mathematical expressions developed by four different authors: Kouwenhoven [2], Gladman [3], Licka et al. [4], and Burnett [5].

The Ashby–Orowan precipitation strengthening is calculated because a term is included in the Gladman and Kouwenhoven expressions.

2. Steels studied

Three medium carbon microalloyed steels, with an almost constant vanadium weight percentage and titanium content were studied. The nitrogen content varied to such a small extent that its influence on the grain size was minimal, although relatively important as regards resistance properties (tensile strength and yield strength).

The chemical composition in weight percentage and parts per million (p.p.m.) for the gases, is shown in Table I.

Steels were prepared as follows: Steel 1 was melted using an electric-arc melting furnace and a vacuum ladle furnace. It was cast under protective slag into 250 mm × 250 mm ingots. Later, Steel 1 was hot rolled to 110 mm square billets. These billets were re-rolled

TABLE I Chemical composition (wt % and p.p.m.)

Steels	C (%)	Mn (%)	Si (%)	S (%)	P (%)	Cr (%)	Ni (%)	Mo (%)	V (%)	Ti (%)	Cu (%)	Sn (%)	Al (%)	N_2 (p.p.m.)	O_2 (p.p.m.)
1	0.29	1.34	0.41	0.026	0.021	0.09	0.10	0.02	0.10	0.003	0.244	0.020	0.029	167	30
2	0.29	1.28	0.34	0.028	0.017	0.13	0.08	0.01	0.09	0.019	0.134	0.015	0.036	106	45
3	0.32	1.39	0.33	0.021	0.015	0.13	0.14	0.03	0.129	0.039	0.129	0.017	0.049	148	57

0022–2461

to 38.5 mm square billets and cooled in air (ensuring that the billets were not stacked). Steels 2 and 3 were melted under a protective atmosphere in an induction furnace. These two steels were air cast into 115 mm × 155 mm ingots. Ingots were rolled to 38.5 mm square billets.

Re-heating and finishing last-rolling temperatures were close to 1230 and 1080 °C, respectively, in all three steels.

3. Forging runs

The deformation parameters corresponding to the fabrication of an automotive connecting rod have been determined [1].

The forging runs are listed in Table II. The first one is a classic sequence and obtains the complete dissolution of the vanadium and titanium carbonitrides and nitrides. The furnace heating temperature used in the second forging run (1373 K) is higher than the com-

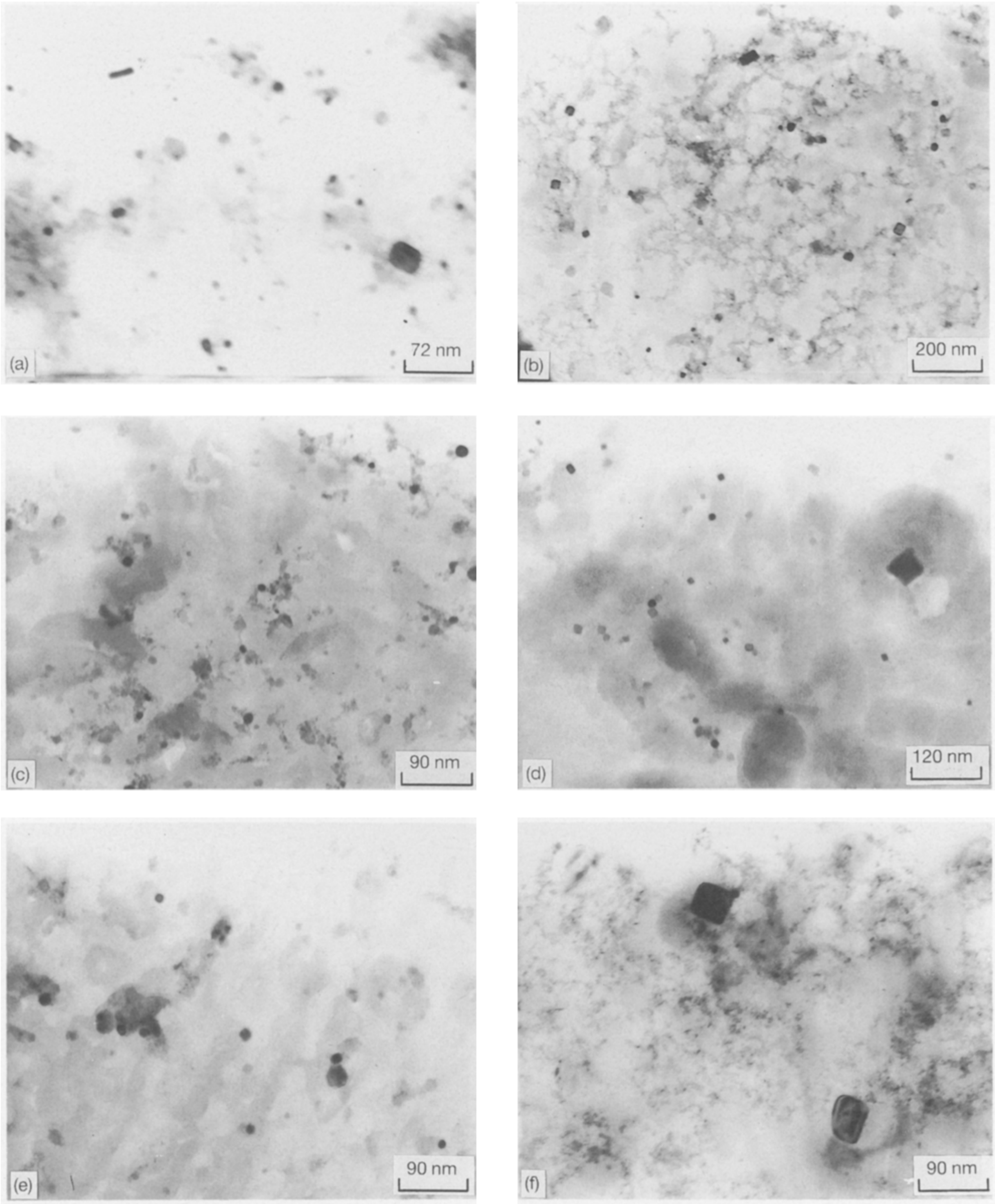

Figure 1 Precipitates. Size and distribution. (a) Steel 1, $T_2 = 1323$ K; (b) Steel 1, $T_2 = 1398$ K; (c) Steel 2, $T_2 = 1323$ K; (d) Steel 2, $T_2 = 1398$ K; (e) Steel 3, $T_2 = 1323$ K; (f) Steel 3, $T_2 = 1398$ K.

TABLE II Temperatures for the two forging runs

Furnace heating (K)	1st run, T(K) $\dot{\varepsilon} = 13.7\,s^{-1}$, $\varepsilon = 1.443$	2nd Run, T(K) $\dot{\varepsilon} = 18.9\,s^{-1}$, $\varepsilon = 0.779$
1523	1453	1398
1373	1353	1323

plete dissolution temperature of the vanadium carbonitrides and nitrides, but it is not so for the titanium ones. That is not important for obtaining the best results because the final hardness is not increased by the titanium precipitates. Its role is only to hinder the austenitic grain growth and therefore to obtain the finest ferritic–pearlitic grain [6, 7].

4. Precipitates

Fig. 1 shows some particle distribution fields. Figs. 2 and 3 show the diffraction results from the precipitates which were Ti,N and Ti (CN) with (V Ti)N and (V Ti)CN. VN and V(CN) probably exist too, but multiple or "prohibited" reflections make it impossible to analyse the vanadium carbonitrides.

Finally, the lamellar pearlitic is shown in Fig. 4.

Steel 2 had a smaller grain size, with a temperature grain coarsening (TGC, temperature at which grains of different sizes appear) of about 1200 °C. This occurs because the precipitates are mainly of titanium and they have a suitable size (~ 10 nm).

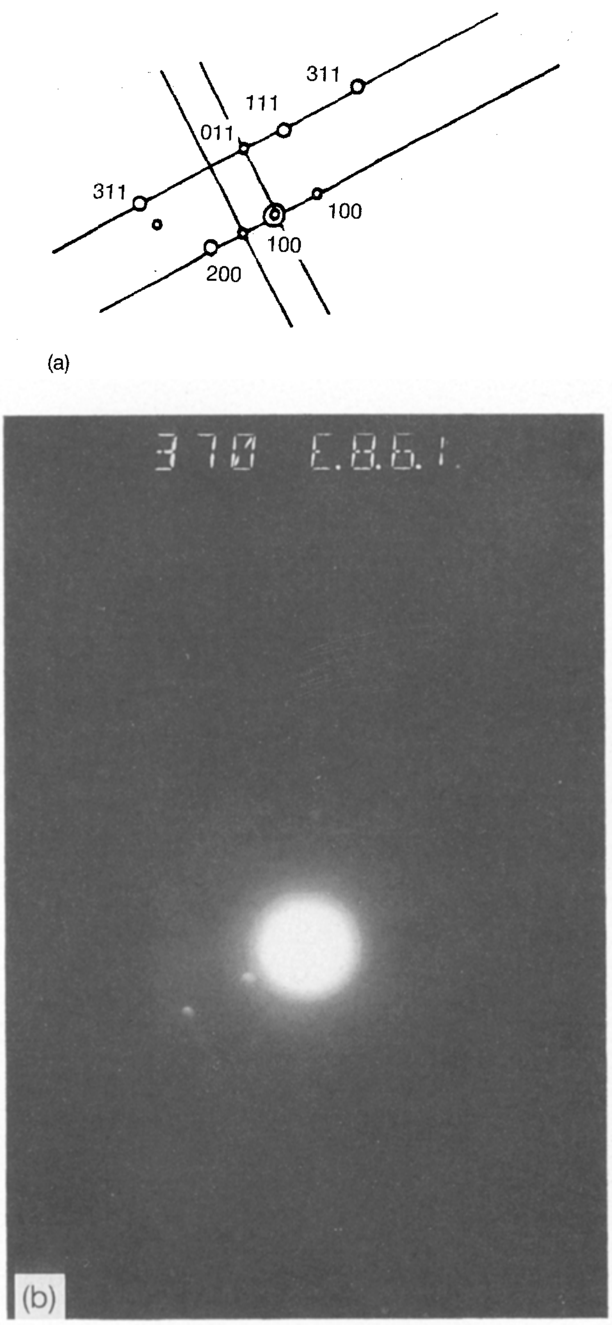

Figure 2 Titanium carbonitrides, diffraction patterns.

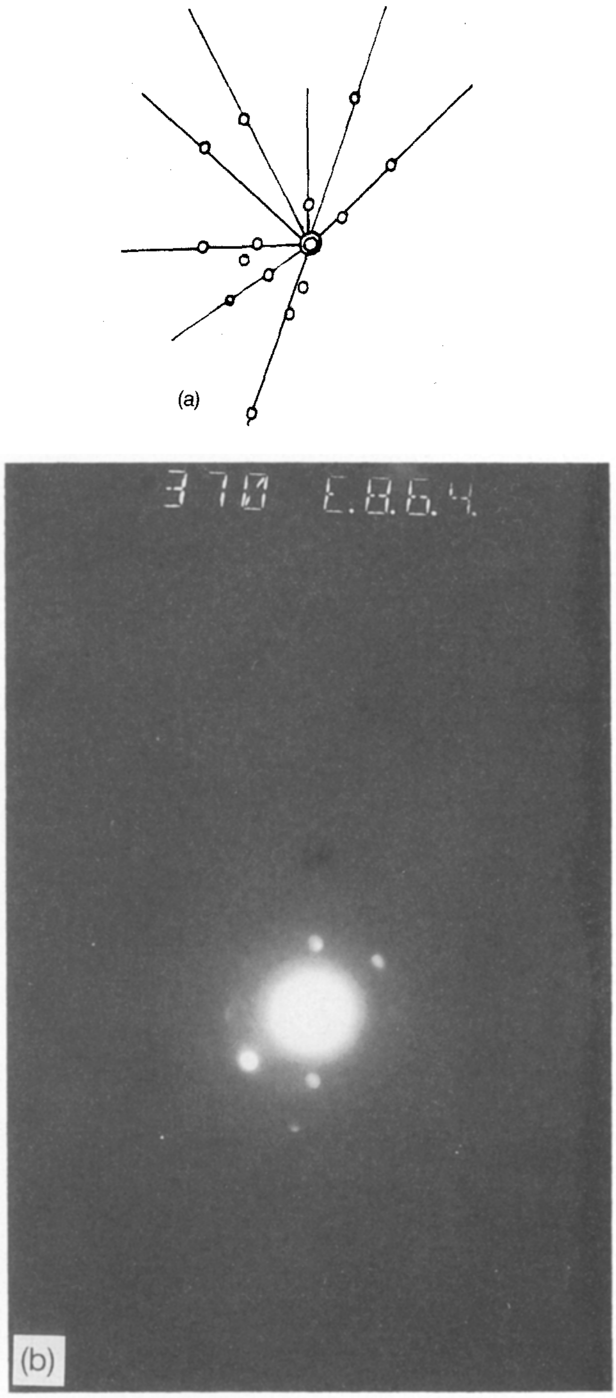

Figure 3 Vanadium carbonitrides, diffraction patterns.

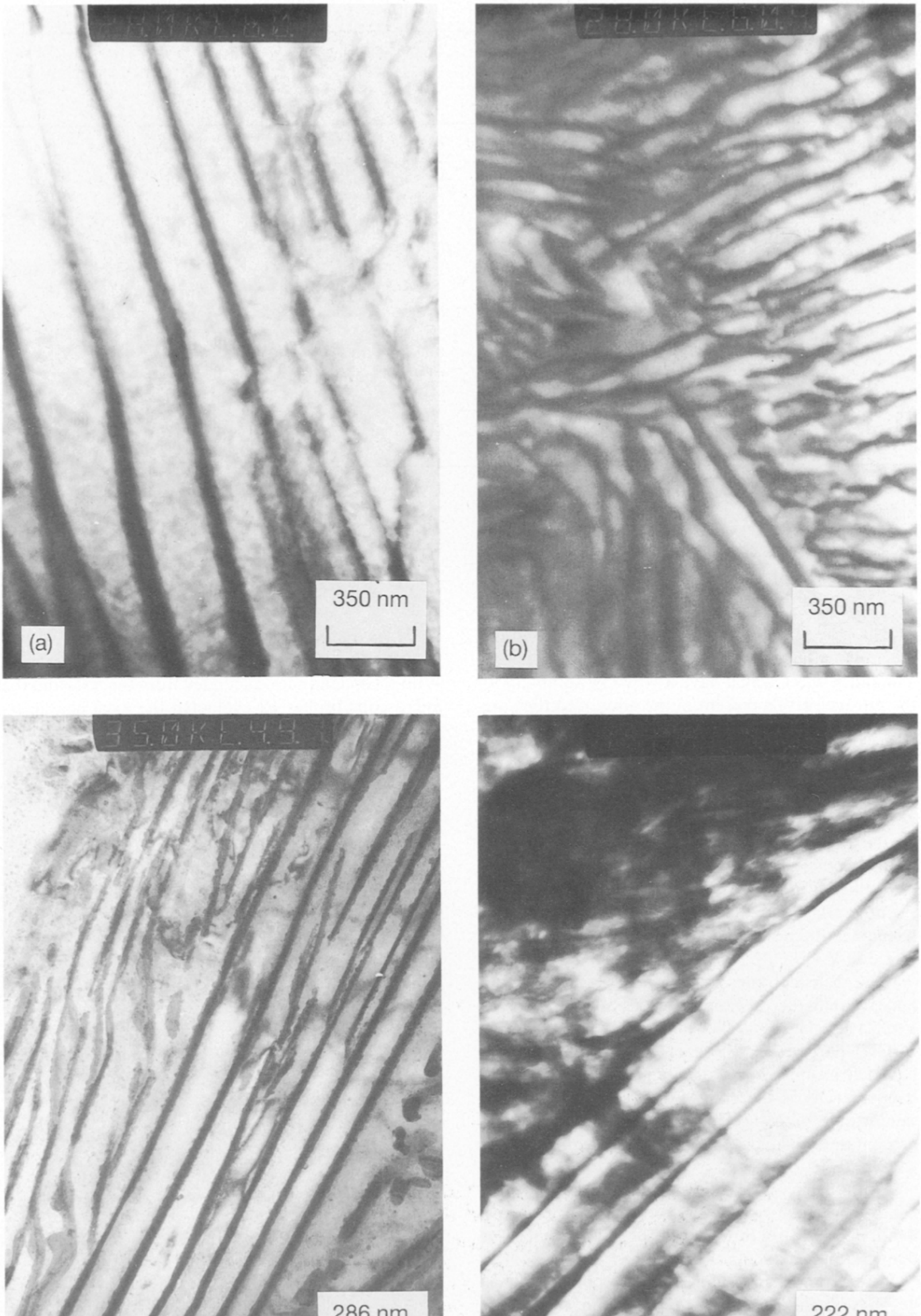

Figure 4 Lamellar pearlitic consistituent for the three steels at different forging temperatures. (a) Steel 1, $T_2 = 1398$ K; (b) Steel 1, $T_2 = 1323$ K; (c) Steel 2, $T_2 = 1323$ K; (d) Steel 3, $T_2 = 1323$ K.

TABLE III Precipitates parameters

Steel	Steel temp. sequences (K)	Number of precipitates	Mean distance between particles (nm)			Precipitate size distribution (%) and mean size, d (nm)					Volume particles fraction
			max.	min.	mean	< 20	20–40	40–60	> 60	d	
1	$T_\gamma = 1523$ $T_2 = 1398$	50	1011	13	322	88% (44 prec.)	10% (5 prec.)	2% (1 prec.)	0%	8.8	0.007
	$T_\gamma = 1373$ $T_2 = 1323$	62	656	5	207	90% (58 prec.)	8% (5 prec.)	2% (1 prec.)	0%	9.2	0.005
2	$T_\gamma = 1523$ $T_2 = 1398$	45	1054	4	333	91% (42 prec.)	9% (3 prec.)	0%	0%	14.3	0.008
	$T_\gamma = 1373$ $T_2 = 1323$	70	750	7	310	97% (68 prec.)	3% (2 prec.)	0%	0%	9.2	0.002
3	$T_\gamma = 1523$ $T_2 = 1398$	2[a]	270	200	240	0%	0%	50% (1 prec.)	50% (2 prec.)	65	0.009
		40[b]	830	10	320	85% (34 prec.)	15% (6 prec.)	0%	0%	10.5	0.006
	$T_\gamma = 1373$ $T_2 = 1323$	4[a]	320	320	320	0%	0%	50% (2 prec.)	50% (2 prec.)	45	0.011
		56[b]	630	14	380	84% (47 prec.)	16% (9 prec.)	0%	0%	9.3	0.004

[a] Segregated zones.
[b] Unsegregated zones.

Alloy 1 has a very low TGC because although its precipitates have an adequate size, they are mainly VN and V(CN), which have a very low solubility for the nitrogen levels present in the alloy, and they precipitate for the most part in ferrite–pearlite instead of austenite.

Alloy 3 exhibits zones where the precipitates have been segregated exceeding the critical size, and they do not inhibit the boundary-grain migration in any way. In the non-segregated zones, the particle sizes are similar to those of Alloy 2, having a higher proportion of VN and V(CN).

Table III shows the precipitates parameters. The factors for the pearlitic component (S, t) are included in Table V.

If we consider the precipitation-strengthening, it appears that the precipitates of the alloy 1 (VN) or V(CN) are the most efficient. In alloy 2, the Ti,N or Ti(CN) particles or those of (V Ti)N or (V Ti)CN have left insufficient nitrogen and vanadium to form V,N or V(CN) in the ferrite. For this reason there is no significative difference in the hardening due to the precipitates when the austenitization temperature is varied.

Alloy 3 behaves in a different way, depending on the zone, or whether or not it is segregated. On the other hand, bainitic structures appear at low austenization temperatures, reducing the toughness.

The interlamellar distance as well as the lath thickness have been calculated for the pearlitic phase. From the values obtained, we can deduce that the interlamellar distance decreases together with the deformation temperature. This occurs because there is a correspondence between lower deformation temperatures and higher cooling velocities during the transformation $\gamma \rightarrow \alpha + P$ with decreasing Ar_3.

5. Resolution of the Hall–Petch equation

With the magnitudes calculated from the tests and the microscope probes we evaluated the most characteristic properties of these steels: stress, yield stress, impact-transition temperature. We used the following expressions:

Ashby–Orowan

$$\sigma_p = 5 \cdot 9 (f/X)^{1/2} \ln \;(X/2.5 \times 10^4) \qquad (1)$$

where σ_p is the precipitation strenghtening (MPa), f the volume particles fraction, and X the mean planar-intercept diameter of a precipitate (μm).

Gladman

$$\sigma_y = \sigma_p + f_\alpha^{1/3}[35 + 58.5\,(\%\text{Mn}) + 17.4\,d^{-1/2}] + (1 - f_\alpha^{1/3})\,[178 + 3.85\,s^{-1/2}] + 63.1 \times (\%\text{Si}) + 425(\%\text{N}_\text{F})^{1/2} \pm 45\,\text{MPa} \qquad (2)$$

$$\sigma_T = \sigma_p + f_\alpha^{1/3}[246 + 1140 \times (\%\text{N}_\text{F})^{1/2} + 18.2\,d^{-1/2}] + (1 - f_\alpha^{1/3}) \times [720 + 3.5\,s^{-1/2}] + 97 \times \%\text{Si} \pm 45\,\text{MPa} \qquad (3)$$

$$\text{ITT} = f_\alpha(-46 - 11.5\,d^{-1/2}) + (1 - f_\alpha) \times (-335 + 5.6\,s^{-1/2} - 13.3\,p^{-1/2}) + (3.48 \times 10^6)t + 48.7\,(\%\text{Si}) + 762\,(\%\text{N}_\text{F}) \pm 30\,^\circ\text{C} \qquad (4)$$

where σ_y is the yield stress (MPa), σ_T the ultimate tensile strength (MPa), ITT the impact-transition temperature (temperature in °C for a Charpy V notch impact toughness = 27 J), f_α the volume ferrite fraction, d the ferrite grain size (nm), s the pearlite interlamellar spacing (nm), t the pearlite lath thickness (nm) and N_F the free nitrogen.

Kouwenhoven equation

$$\sigma_y = 54 f_\alpha + [380 + 94\,(\%\text{Mn}) f_p + 72\,(\%\text{Si}) + 26 f_\alpha (d^{-1/2}) \quad (5)$$

where f_p is the volume pearlite fraction.

Licka *et al.*'s equation

$$\sigma_T = f_\alpha^{1/3} [246 + 18.2 d^{-1/2}] + (1 - f_\alpha^{1/3}) \times [720 + 3.5 s^{-1/2}] + 97 \times (\%\text{Si}) + 1047 \times (\%\text{V}) + 2294 \times (\%\text{N}) \quad (6)$$

$$\sigma_y = f_\alpha^{1/3} [35 + 58\,\%\text{Mn} + 17.4 d^{-1/2}] + (1 - f_\alpha^{1/3}) [178 + 3.8 s^{-1/2}] + 63 \times \%\text{Si} + 3535\,([\text{V}][\text{N}])^{1/2} \quad (7)$$

$$\text{ITT} = -(19 + 11.5 d^{-1/2}) + 44 \times \%\text{Si} + 2.2\,(\%\text{pearlite}) + 919\,(\text{VN})^{1/2} \quad (8)$$

Burnett equation

$$\sigma_T = 294 + \%\text{ferrite}\,[0.743\,(\ln \text{cooling rate})\ {}^\circ\text{C min}^{-1}] + \%\text{pearlite}\,[3.80 (p^{-1/2}) + 1.41 \times s^{-1/2}] + 104\,\%\text{Mn} \quad (9)$$

$$\sigma_y = 102 + \%\text{ferrite}\,[0.833\,(\ln \text{cooling rate}]\ {}^\circ\text{C min}^{-1}] - 1.50 \times d^{-1/2}] + \%\text{pearlite}\,(2.02 \times p^{-1/2} + 1.47 s^{-1/2}) + 68 \times \%\text{Mn} \quad (10)$$

p represents the pearlite colony size (μm). The other symbols are the same as in the Gladman equation but are also in micrometres.

The data obtained are shown in Tables III and IV together with the expected results for each model. All the actual results obtained from the connecting rods are also shown in Table V.

TABLE IV Ashby–Orowan precipitation strengthening

Steels	Forging runs (K)	f	d (nm)	X (nm)	σ_p (MPa)
1	$T_\gamma = 1523$, $T_2 = 1398$	0.007	8.8	7.85	214
	$T_\gamma = 1373$, $T_2 = 1323$	0.005	9.2	8.2	178
2	$T_\gamma = 1523$, $T_2 = 1398$	0.008	14.3	12.7	115
	$T_\gamma = 1373$, $T_2 = 1323$	0.002	9.2	9.2	113
3	$T_\gamma = 1523$, $T_2 = 1398$	0.009	65	58.0	52
	$T_\gamma = 1373$, $T_2 = 1323$	0.011	52	40.1	74

6. Discussion

The hardness with a high content of titanium increases, not by precipitation but because of the appearance of bainitic structures, which is fateful for the impact toughness characteristics.

TABLE V Structural characteristics and theoretical previous for the three steels studied

T, 2nd run (K)	f_α	f_p	d_α (μm)	s (μm)	p (μm)	t (μm)	σ_y	σ	ITT (°C)	Model[a]
1398	0.44	0.56	11	0.15	20	23	583	855	23	1
							659	–	–	2
							499	742	50	3
							607	842	–	4
1323	0.46	0.54	8	0.13	12	11	573	827	2	1
							639	–	–	2
							524	761	26	3
							630	869	–	4
1398	0.47	0.53	8.5	0.20	18	16	477	725	10	1
							563	–	–	2
							461	710	15	3
							578	811	–	4
1323	0.49	0.51	7.5	0.12	9	19	499	734	–5	1
							566	–	–	2
							481	729	4	3
							637	876	–	4
1398	0.34	0.66	9	0.14	18	18	566	829	48	1
							633	–	–	2
							623	812	60	3
							624	868	–	4
1323	0.39	0.34 + bainite								

[a] 1, Gladman *et al.*; 2, Kouwenhoven; 3, Licka *et al.*; 4, Burnett.

TABLE VI Experimental results for the three steels studied

Steels	Forging runs (K)	MPa	$\sigma_{0.2}$ (MPa)	H_{V10}	d_α (μm)	p (μm)	V_α	V_p	ITT (°C)
1	$T_\gamma = 1523$	860	626	269	11	20	0.44	0.56	15
	$T_2 = 1398$								
	$T_\gamma = 1373$	870	633	271	8	12	0.46	0.54	− 7
0.003 Ti	$T_2 = 1323$								
2	$T_\gamma = 1523$	748	491	243	8.5	18	0.47	0.53	− 5
	$T_2 = 1398$								
	$T_\gamma = 1373$	760	510	233	7.5	9	0.51	0.49	− 20
0.019 Ti	$T_2 = 1323$								
3	$T_\gamma = 1523$	870	598	290	9	19	0.34	0.66	69
	$T_2 = 1398$								
	$T_\gamma = 1373$	850	569	270	8	11	0.39	0.34 +	36
0.039 Ti	$T_2 = 1323$							bainite	

The ultimate tensile strength values and the yield strength are lower in Alloy 2, due to the loss of nitrogen and vanadium as hardening elements, because of the formation of titanium composites [1], although, it has optimum toughness characteristics.

7. Conclusion

From the three alloys studied, Alloy 2 (V = 0.10%, Ti = 0.019%) has better toughness characteristics. Its low strength level can be improved by changing its chemical composition, for example by increasing the percentage of vanadium and nitrogen.

The mechanical properties increase with a lower deformation temperature.

The Gladman equations provide better results, but their confidence limits (± 45 MPa, ± 30 °C) are excessive, especially for the impact transition temperature.

References

1. F. PEÑALBA, Desitation Complutense University of Madrid, Physics Faculty (1991).
2. H. J. KOUWENHOVEN, *Trans. ASM* **62** (1969) 437.
3. T. GLADMAN, D. DULIEU and I. McIVOR, in "Microalloying '75 Proceedings", edited by M. Korchynsky (Union Carbide Corporation, New York, 1977) pp. 32–57.
4. S. LICKA, J. WOZNIAK. M. KOSAR and T. PRNKA, "Thermomechanical Processing of Microalloyed Austenite" (Metallurgical Society of AIME, Pittsburgh PA, 1987) pp. 521–8.
5. M. E. BURNETT, "Fundamentals of Microalloying Forging Steels" (Metallurgical Society of AIME, Pittsburgh PA, 1987) pp. 601–26.
6. F. PEÑALBA, M. CARSÍ, C. GARCÍA and F. ZAPIRAIN, *Mem. Sci. Rev. Met.* **2** (1991) 77.
7. F. PEÑALBA, M. CARSÍ, C. GARCÍA, M. P. de ANDRÉS and F. ZAPIRAIN, *ISI J. Int.* **32** (1992) 232.

Received 29 June 1992
and accepted 20 April 1993